(12) INTERNATIONAL APPLICATION PUBLISHED UNDER THE PATENT COOPERATION TREATY (PCT)

(19) World Intellectual Property Organization
International Bureau

(43) International Publication Date
26 June 2025 (26.06.2025)

WIPO | PCT

(10) International Publication Number
WO 2025/133673 A2

(51) International Patent Classification:
Not classified

(21) International Application Number:
PCT/IB2023/062856

(22) International Filing Date:
18 December 2023 (18.12.2023)

(25) Filing Language: English

(26) Publication Language: English

(71) Applicant: **EQ TECH ENERGY CO. LTD.** [TH/TH]; 399/22 Village No.8, Suan Luang Sub-district, Krathum Baen district, Samut Sakhon, 74000 (TH).

(72) Inventors: **MEEVASANA, Worawat**; c/o EQ Tech Energy Co. Ltd., 399/22 Village No.8, Suan Luang Sub-district, Krathum Baen district, Samut Sakhon, 74000 (TH). **WONGPRATAT, Unchista**; c/o EQ Tech Energy Co. Ltd., 399/22 Village No.8, Suan Luang Sub-district, Krathum Baen district, Samut Sakhon, 74000 (TH). **MUSIKAJAROEN, Supansa**; c/o EQ Tech Energy Co. Ltd., 399/22 Village No.8, Suan Luang Sub-district, Krathum Baen district, Samut Sakhon, 74000 (TH).

(74) Agent: **VACHANAVUTTIVONG, Darani**; Tilleke & Gibbins International Limited, No. 1011, Supalai Grand Tower, 26th Floor, Rama 3 Road, Chongnonsi Sub-District, Yannawa District, Bangkok, 10120 (TH).

(81) Designated States *(unless otherwise indicated, for every kind of national protection available)*: AE, AG, AL, AM, AO, AT, AU, AZ, BA, BB, BG, BH, BN, BR, BW, BY, BZ, CA, CH, CL, CN, CO, CR, CU, CV, CZ, DE, DJ, DK, DM, DO, DZ, EC, EE, EG, ES, FI, GB, GD, GE, GH, GM, GT, HN, HR, HU, ID, IL, IN, IQ, IR, IS, IT, JM, JO, JP, KE, KG, KH, KN, KP, KR, KW, KZ, LA, LC, LK, LR, LS, LU, LY, MA, MD, MG, MK, MN, MU, MW, MX, MY, MZ, NA, NG, NI, NO, NZ, OM, PA, PE, PG, PH, PL, PT, QA, RO, RS, RU, RW, SA, SC, SD, SE, SG, SK, SL, ST, SV, SY, TH, TJ, TM, TN, TR, TT, TZ, UA, UG, US, UZ, VC, VN, WS, ZA, ZM, ZW.

(84) Designated States *(unless otherwise indicated, for every kind of regional protection available)*: ARIPO (BW, CV, GH, GM, KE, LR, LS, MW, MZ, NA, RW, SC, SD, SL, ST, SZ, TZ, UG, ZM, ZW), Eurasian (AM, AZ, BY, KG, KZ, RU, TJ, TM), European (AL, AT, BE, BG, CH, CY, CZ, DE, DK, EE, ES, FI, FR, GB, GR, HR, HU, IE, IS, IT, LT, LU, LV, MC, ME, MK, MT, NL, NO, PL, PT, RO, RS, SE, SI, SK, SM, TR), OAPI (BF, BJ, CF, CG, CI, CM, GA, GN, GQ, GW, KM, ML, MR, NE, SN, TD, TG).

(54) Title: COATING OF AN ELECTRODE

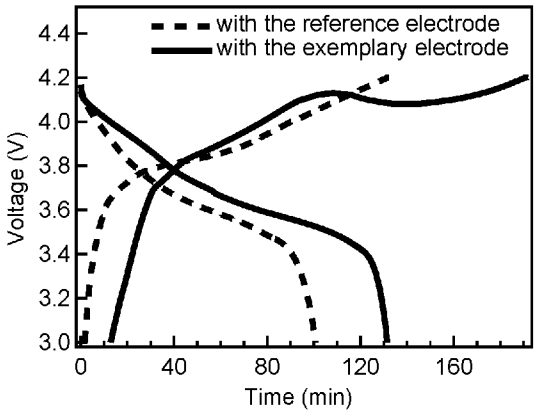

FIG. 5

(57) Abstract: Aspects in accordance with the present invention pertain to an active coating of an electrode active material, said active coating having a thickness of 1 nanometer – 1 micrometer and comprising a transition metal oxide, said active coating imparting, to the electrode active material upon which said active coating is deposited, a negative rate of μ over n, wherein: said μ represents a chemical potential; said n represents a number of electron per a unit area; and said negative rate is between 0 and -5.39 x 10-^{8} millielectronvolt per electron per cm^{2}.

[Continued on next page]

WO 2025/133673 A2

Declarations under Rule 4.17:

— *as to the identity of the inventor (Rule 4.17(i))*
— *as to applicant's entitlement to apply for and be granted a patent (Rule 4.17(ii))*
— *of inventorship (Rule 4.17(iv))*

Published:

— *without international search report and to be republished upon receipt of that report (Rule 48.2(g))*
— *in black and white; the international application as filed contained color or greyscale and is available for download from PATENTSCOPE*

TITLE OF THE INVENTION
COATING OF AN ELECTRODE

FIELD OF THE INVENTION

The present invention relates to a coating, particularly a coating of an electrode, and more particularly where said coating modifies the electrode's electrochemical properties.

BACKGROUND OF THE INVENTION

Electrodes are essential components of energy storage devices, particularly those involving electrochemistry. Examples of such energy storage devices are capacitors, supercapacitors, and batteries, particularly lithium-ion batteries.

Selection of the electrode active material depends on the type of that electrode, i.e. whether the electrode is a cathode (positive electrode) or an anode (negative electrode). Conventional cathode active materials include lithium cobalt oxide ($LiCoO_2$, LCO), lithium manganese oxide ($LiMn_2O$, LMO), lithium nickel-cobalt-aluminum oxide ($LiNiCoAlO_2$, NCA), lithium nickel-manganese-cobalt oxide ($LiNiMnCoO_2$, NMC), and lithium iron phosphate ($LiFePO_4$, LFP); whereas conventional anode active materials include graphite, silicon, iron, and carbon steel.

Many attempts have been made to improve the electrode's electrochemical properties, which are crucial for the working of the energy storage device. In general, the improvement may be made by way of enhancing an existing electrode active material or finding a new electrode active material.

An example of such attempts is US 2019/0207202 A1, which proposes a positive electrode, a method for preparing the positive electrode and an electrochemical device. Configurations of the positive electrode active material layer according to US 2019/0207202 A1, including the thickness and porosity of the inorganic layer arranged thereupon, aim to improve the positive electrode's wettability with the electrolyte, which consequently improves the cycle performance, high-temperature storage performance and safety of the resulting electrochemical device.

Further, Nathabumroong et al., Sci Rep 10, 5153 (2020), reported negative electronic compressibility and capacitance enhancement exhibited by lightly-doped metal oxide $Bi_{0.95}La_{0.05}FeO_3$ (BLFO) in its compressed ceramics pellets form. The study showed potential of at least BLFO for use as an active electrode material.

SUMMARY OF THE INVENTION

An object of the present invention is to provide an active coating of an electrode active material capable of imparting the electrode active material with negative electronic compressibility, thereby enhancing the energy storage capacity of that electrode active material. Also, an object of the present invention is to provide an energy storage device to which the electrode active material coated with said active coating is applied.

In the first aspect, an embodiment is an active coating of an electrode active material. Said active coating has a thickness of 1 nanometer – 1 micrometer and comprising a transition metal oxide. Said active coating imparts, to the electrode active material upon which said active coating is deposited, a negative rate of μ over n, wherein: said μ represents a chemical potential; said n represents a number of electrons per a unit area; and said negative rate is between 0 and -5.39×10^{-8} millielectronvolt per electron per cm^2.

The present inventors have found that, by applying the active coating according to the embodiments described herein, the resulting electrode active material exhibits a surprising extent of negative electronic compressibility: the negative rate of μ over n between 0 and -5.39×10^{-8} millielectronvolt per electron per cm^2.

Preferably, said transition metal oxide is doped with at least one metal dopant.

Because the favorable negative rate of μ over n is a function of n, doping can be used to fine-tune this rate and energy density. Species and proportion of metal dopant in the active coating affect this fine-tuning. The present inventors have found that certain groups/species and proportions of metal dopants in the active coating material caused the negative rate of μ over n to be nearly equal to the increase in chemical potential, resulting in the average slope of μ over n in the charging phase being substantially close to 0, thereby exhibiting the high energy density. Comparison between Exemplary Embodiment Nos. 8 and 9, to be described further below, should illustrate this fine-tuning effect.

More preferably, said metal dopant is a transition metal element or a post-transition metal element.

Even more preferably, said metal dopant is selected from a group of niobium (Nb), indium (In) and copper (Cu).

Preferably, La and/or Cu is selected as a metal dopant for doping $BiFeO_3$. Also preferably, Co, Nb and/or In is selected as a metal dopant for doping a titanate-based material.

Preferably, the transition metal oxide is selected from a group of bismuth ferrite ($BiFeO_3$, BFO), nickel (II) oxide (NiO), and barium titanate (BaTiO3).

Most preferably, the transition metal oxide that is doped with at least one metal dopant is $Bi_{0.95}$ $Cu_{0.05}$ FeO_3.

In an embodiment, the doping is carried out in order to optimize the negative rate of μ over n, such that said negative rate of μ over n corresponds to a host energy storage where the active coating is applied.

Optionally, the active coating is applied to the electrode active material by physical vapor deposition.

The electrode active material, upon which the active coating in accordance with any of the above embodiments is applied, may be used as a component of any known energy storage device that is part of a capacitor (in particular a supercapacitor and the like), or a battery (in particular a lithium-ion battery and the like). Said energy storage device may take the form of a coin cell or a cylindrical cell of a capacitor or a battery.

In the second aspect, an embodiment is the energy storage device that is part of a capacitor (in particular a supercapacitor and the like), or a battery (in particular a lithium-ion battery and the like) that comprises an electrode active material upon which the active coating in accordance with any of the above embodiments of the first aspect is deposited.

Further below, the present inventors have provided description and drawings of exemplary embodiments where said energy storage device takes the form of a coin cell and a cylindrical cell of a capacitor or a battery.

BRIEF DESCRIPTION OF DRAWINGS

The principle of the present invention and its advantages will become apparent in the following description, taking into consideration the accompanying drawings in which:

Fig. 1 shows a schematic diagram of a supercapacitor having a coin cell configuration according to an exemplary embodiment (not to scale).

Fig. 2 shows a schematic diagram of a supercapacitor having a cylindrical cell configuration according to an exemplary embodiment (not to scale).

Fig. 3 shows a schematic diagram of a battery having a coin cell configuration according to an exemplary embodiment (not to scale).

Fig. 4 shows a schematic diagram of a battery having a cylindrical cell configuration according to an exemplary embodiment (not to scale).

Fig. 5 shows the change of voltage (V) over time (minutes) of an NMC electrode coated with an active coating comprising Cu-doped $BiFeO_3$ according to Exemplary Embodiment No. 1.

Fig. 6A shows the change of the chemical potential μ as a function of the electron density *n2D* of an electrode active material coated with an active coating comprising $BiFeO_3$ according to Exemplary Embodiment No. 2.

Fig. 6B shows the rate of change of the chemical potential over the electron density ($d\mu/dn$) as a function of the electron density *n2D* of an electrode active material coated with an active coating comprising $BiFeO_3$ according to Exemplary Embodiment No. 2.

Fig. 7 shows the percentage of energy density increase (%) as a function of active coating thickness in a Li-ion battery-based lithium-nickel-manganese-cobalt oxide ($LiNiMnCoO_2$, NMC) electrode coated with Cu-doped $BiFeO_3$ thin film according to Exemplary Embodiment No. 3.

Fig. 8A shows the change of voltage (V) over time (minutes) of a supercapacitor comprising reference electrodes and another supercapacitor comprising electrodes according to Exemplary Embodiment No. 4.

Fig. 8B shows the change of energy density (Wh/kg) over cycles of charge/discharge of a supercapacitor comprising reference electrodes and another supercapacitor comprising electrodes according to Exemplary Embodiment No. 4.

Fig. 9A shows the change of voltage (V) over time (minutes) of a supercapacitor comprising reference electrodes and another supercapacitor comprising electrodes according to Exemplary Embodiment No. 5.

Fig. 9B shows the change of energy density (Wh/kg) over cycles of charge/discharge of a supercapacitor comprising reference electrodes and another supercapacitor comprising electrodes according to Exemplary Embodiment No. 5.

Fig. 10A shows the change of voltage (V) over time (minutes) of a supercapacitor comprising reference electrodes and another supercapacitor comprising electrodes according to Exemplary Embodiment No. 6.

Fig. 10B shows the change of energy density (Wh/kg) over cycles of charge/discharge of a supercapacitor comprising reference electrodes and another supercapacitor comprising electrodes according to Exemplary Embodiment No. 6.

Fig. 11A shows the change of voltage (V) over time (minutes) of a lithium-ion battery comprising reference electrodes and another lithium-ion battery comprising electrodes according to Exemplary Embodiment No. 7.

Fig. 11B shows the change of energy density (Wh/kg) over cycles of charge/discharge of a lithium-ion battery comprising reference electrodes and another lithium-ion battery comprising electrodes according to Exemplary Embodiment No. 7.

Fig. 12A shows the change of voltage (V) over time (minutes) of a lithium-ion battery comprising reference electrodes and another lithium-ion battery comprising electrodes according to Exemplary Embodiment No. 8.

Fig. 12B shows the change of energy density (Wh/kg) over cycles of charge/discharge of a lithium-ion battery comprising reference electrodes and another lithium-ion battery comprising electrodes according to Exemplary Embodiment No. 8.

Fig. 13A shows the change of voltage (V) over time (minutes) of a lithium-ion battery comprising reference electrodes and another lithium-ion battery comprising electrodes according to Exemplary Embodiment No. 9.

Fig. 13B shows the change of energy density (Wh/kg) over cycles of charge/discharge of a lithium-ion battery comprising reference electrodes and another lithium-ion battery comprising electrodes according to Exemplary Embodiment No. 9.

Fig. 14A shows the change of voltage (V) over time (minutes) of a lithium-ion battery comprising reference electrodes and another lithium-ion battery comprising electrodes according to Exemplary Embodiment No. 10.

Fig. 14B shows the change of energy density (Wh/kg) over cycles of charge/discharge of a lithium-ion battery comprising reference electrodes and another lithium-ion battery comprising electrodes according to Exemplary Embodiment No. 10.

Fig. 15A shows the change of voltage (V) over time (minutes) of a lithium-ion battery comprising reference electrodes and another lithium-ion battery comprising electrodes according to Exemplary Embodiment No. 11.

Fig. 15B shows the change of energy density (Wh/kg) over cycles of charge/discharge of a lithium-ion battery comprising reference electrodes and another lithium-ion battery comprising electrodes according to Exemplary Embodiment No. 11.

DETAILED DESCRIPTION OF EMBODIMENTS OF THE INVENTION

It is to be understood that the following detailed description will be directed to embodiments, provided as examples for illustrating the concept of the present invention only. The present invention is in fact not limited to particular embodiments described, as such may, of course, vary. It is also to be understood that the terminology used herein is for the purpose of describing particular embodiments only, and is not intended to be limiting, since the scope of this invention will be limited only by the appended claims.

The detailed description of the invention is divided into various sections only for the reader's convenience and disclosure found in any section may be combined with that in another section.

Unless defined otherwise, all technical and scientific terms used herein have the same meaning as commonly understood by one of ordinary skills in the art to which this invention belongs.

It must be noted that as used herein and in the appended claims, the singular forms "a", "an", and "the" include plural referents unless the context clearly dictates otherwise.

The term "about" when used before a numerical designation, e.g., dimensions, time, amount, and such other, including a range, indicates approximations which may vary by (+) or (-) 10 %, 5 % or 1 %, or any sub-range or sub-value there between.

"Comprising" or "comprises" is intended to mean that the compositions and methods include the recited elements, but not excluding others. "Consisting essentially of" when used to define compositions and methods, shall mean excluding other elements of any essential significance to the combination for the stated purpose. Thus, a device or method consisting essentially of the elements as defined herein would not exclude other materials or steps that do not materially affect the basic and novel characteristic(s) of the claimed invention. "Consisting of" shall mean excluding more

than trace elements of other ingredients and substantial method steps. Embodiments defined by each of these transition terms are within the scope of this invention.

"Electron density" refers to the number of electrons per unit area.

Active Coating

Being preferably coated upon the electrode active material, an active coating modifies the electrode active material's rate of μ over n (i.e., the chemical shift). Exemplary materials for the active coating include copper-doped bismuth ferrite (Cu-doped BFO).

In an embodiment comprising a protective coating (see the next section for detail), the active coating is preferably applied to the electrode active material before the protective coating.

Protective coating

Being preferably coated upon the active coating, the protective coating protects the active coating from chemical attacks during the charge and discharge. Even more preferably, the protective coating is a conductive metal, preferably copper (Cu), nickel (Ni), or aluminum (Al) or their alloy, which helps reduce the electrode active material's electrical resistance. The reduction of electrode active material's electrical resistance is favorable to its performance according to the concept of the present invention. The protective coating may be coated preferably on the active coating that is coated upon either the anode or cathode active material (see also description on cathode and anode active materials in the next section).

Electrode Active Materials

The coating according to any of the embodiments may be applied to an electrode active material (i.e., substrate for coating) which may be a cathode active material or an anode active material. The electrode active material may be any commercially available material that is conventionally known for the purpose. Exemplary electrode active materials are carbon-based material (preferred for an anode) and lithium nickel-manganese-cobalt oxide (LiNiMnCoO2, NMC) (preferred for a cathode).

Coating Process

The coating according to any of the embodiments may be applied to the electrode active material by any known process. Physical vapor deposition (PVD) is one of the preferred coating processes. In the following Exemplary Embodiments, the coatings were applied to the electrode active materials by sputtering process, which is a variant of physical vapor deposition.

Specifically, in the Exemplary Embodiments, each of the sputtering processes that were carried out in order to apply the coatings to the electrode active materials was divided into two phases: the sputtering for forming an active coating, and the sputtering for forming a protective coating.

Preferably, the sputtering for forming the active coating was applied by radio frequency (RF) magnetron sputtering. The electrode active materials used in the Exemplary Embodiments had the area of 100 cm^2, for which the power was set to be in the range of 80 – 200 Watts (W) and the deposition time was set to be within 30 seconds to 30 minutes. The reactive gas was a mixture consisting essentially of argon (Ar) and oxygen (O_2). The process was run at the room temperature (RT) under the pressure in the range of 1 – 5 Pascal (Pa).

Also preferably, the sputtering for forming the protective coating was then applied by direct current (DC) sputtering. In the below Exemplary Embodiments, the protective coatings were formed by sputtering conductive metal materials which were preferably copper (Cu), nickel (Ni), and aluminum (Al). For the 100-cm^2 electrode active materials used in the Exemplary Embodiments, the power was set to be in the range of 20 – 50 Watts (W) and the deposition time was set to be within 1 – 5 minutes. The reactive gas was a mixture consisting essentially of argon (Ar). The process was run under the pressure in the range of 0.5 – 2.0 Pascal (Pa), and at the room temperature (RT).

EXEMPLARY EMBODIMENTS

To support the technical characteristics of embodiments according to the present invention, the present inventors have carried out Exemplary Embodiment Nos. 1 –3 to observe the negative rates of μ over n of electrode active materials coated with different active coatings, and further Exemplary Embodiment Nos. 4 – 11 to observe the energy density of energy storage devices to which the said electrode active materials were applied.

In all the following Exemplary Embodiments, an indication of "Cu-doped $BiFeO_3$" refers to $Bi_{0.95}Cu_{0.05}FeO_3$, and an indication of "Indium-Niobium-doped TiO_2" refers to $In_{0.5}Nb_{0.5}TiO_2$.

Table 1 below sets out the specifics of Exemplary Embodiment Nos. 1 – 3 in addition to the preceding general description.

Table 1

Exemplary Embodiment No.	1		2		3	
COATING OF EXEMPLARY ELECTRODE	Active coating	Protective coating	Active coating	Protective coating	Active coating	Protective coating
(1) Substrate (i.e. electrode active material)	NMC		Carbon-based, NMC		NMC	
(2) Coating material	Cu-doped BiFeO3	Cu	BiFeO3	Cu	Cu-doped BiFeO3	Cu
(3) Sputtering source	RF	DC	RF	DC	RF	DC
(4) Operating pressure (Pa)	1.4 ± 0.3	1.0 ± 0.2	0.4 ± 0.3, 1.5 ± 0.3	1 ± 0.2	1.4 ± 0.3	1.0 ± 0.2
(5) Power (W)	100	20	100, 100	20	100	20
(6) Flow rate of the reactive gas (Ar:O2) (sccm)	12:4	5:0	16:4, 12:4	5:0	12:4	5:0
(7) Deposition time (minutes)	30	2	1, 1	2	0.5 - 5.0	2
(8) Substrate temperature (°C)	RT	RT	RT, RT	RT	RT	RT
(9) Thickness (nm)	200	N/A	7, 7	N/A	3.0 - 35.0	N/A

Further, the energy storage devices involved in Exemplary Embodiment Nos. 4 – 11 were supercapacitors and batteries. Their electrode configurations were either coin cells or cylindrical cells. Where the type of energy storage device and/or electrode configuration was mentioned in connection with the below Exemplary Embodiment Nos. 4 – 11, such device/electrode configurations followed the particulars according to Figs. 1 – 4 and their respective description. Those particulars do not limit the scope of the present invention.

Supercapacitor, Coin Cell

Fig. 1 shows a schematic diagram of a supercapacitor having a coin cell configuration 100. The supercapacitor 100 comprises, from its positive terminal to its negative terminal, a positive cap 112, a cathode spring 114, a cathode spacer 116, a cathode 118, a separator 120, an anode 132, an anode spacer 134, and a negative cap 136. The supercapacitor 100 can be assembled by these components starting from the negative cap 136, mounted by the anode spacer 134 and the by the anode 132. Then the separator 120 is interposed between the anode 132 and the cathode 118 to prevent a short circuit current. Finally, the cathode spacer 116, the cathode spring 114, and the positive cap 112 are disposed to top the supercapacitor 100.

In the respective exemplary embodiment, the positive cap 112 was constructed of stainless steel with a dimension of 20 mm × 3.2 mm and a weight of 3.40 g. The cathode spring 114 was constructed of stainless steel with a dimension of 14.5 mm (OD) × 10.25 mm (ID) × 1.2 mm (height) and a weight of 2.83 g. The cathode spacer 116 was constructed of stainless steel with a dimension of 15.8 mm × 1 mm (thickness) and a weight of 2.83 g. The cathode 118 and the anode 132 were constructed of the same electrode active material as specified in the respective exemplary embodiment, and one or both of the cathode 118 and the anode 132 may be coated with a coating material and by the process parameters as specified in the respective exemplary embodiment. The separator 120 was constructed of cellulose fibers with a diameter of 2 cm for coin cell assembly. The anode spacer 134 was constructed of stainless steel with a dimension of 15.8 mm × 1 mm (thickness) and a weight of 2.83 g. And the negative cap 136 was constructed of stainless steel with a dimension of 20 mm × 3.2 mm and a weight of 3.40 g.

Supercapacitor, Cylindrical Cell

Fig. 2 shows a schematic diagram of a supercapacitor having a cylindrical cell configuration 200. The supercapacitor 200 comprises, from its exterior to its core, an enclosure 210, an anode 220,

a separator 230, a cathode 240, and a core 250. The supercapacitor 200 can be assembled by rolling the enclosure 210 as a set of the anode 220, the cathode 240, and the separator, 230 into the core 250.

In the respective exemplary embodiment, the enclosure 210 was constructed of an aluminum foil with a thickness of 1 mm. The anode 220 and the cathode 240 were constructed of the same electrode active material as specified in the respective exemplary embodiment, and one or both of the anode 220 and the cathode 240 may be coated with a coating material and by the process parameters as specified in the respective exemplary embodiment. The separator 230 was constructed of polypropylene (PP) with a length of 100 cm for cylindrical cell assembly. And the core 250 was constructed of stainless steel with a dimension of 18 (OD) mm × 17.5 mm (ID) × 67 mm (height).

Battery, Coin Cell

Fig. 3 shows a schematic diagram of a battery having a coin cell configuration 300. This battery 300 is a lithium-ion (Li-ion) battery. The battery 300 comprises, from its positive terminal to its negative terminal, a positive cap 312, a cathode spring 314, a cathode spacer 316, a cathode 318, a separator 320, an anode 332, an anode spacer 334, and a negative cap 336. The battery 300 can be assembled by these components starting from the negative cap 336, mounted by the anode spacer 334 and the anode 332. Then the separator 320 is interposed between the anode 332 (negative electrode; graphite) and the cathode 318 (positive electrode; NMC) to prevent a short circuit current. Finally, the cathode spacer 316, the cathode spring 314, and the positive cap 312 are disposed to top the battery 300.

In the respective exemplary embodiment, the positive cap 312 was constructed of stainless steel with a dimension of 20 mm × 3.2 mm and a weight of 3.40 g. The cathode spring 314 was constructed of stainless steel with a dimension of 14.5 mm (O.D) × 10.25 mm (I.D) × 1.2 mm (height) and a weight of 2.83 g. The cathode spacer 316 was constructed of stainless steel with a dimension of 15.8 mm × 1 mm (thickness) and a weight of 2.83 g. The cathode 318 was constructed of the electrode active material as specified in the respective exemplary embodiment and may be coated with a coating material and by the process parameters as specified in the respective exemplary embodiment. The separator 320 was constructed of polypropylene (PP) with a diameter of 2 cm for coin cell assembly. The anode 332 was constructed essentially of graphite. The anode spacer 334 was constructed of stainless steel with a dimension of 15.8 mm × 1 mm (thickness) and

a weight of 2.83 g. And the negative cap 336 was constructed of stainless steel with a dimension of 20 mm × 3.2 mm and a weight of 3.40 g.

Battery, Cylindrical Cell

Fig. 4 shows a schematic diagram of a battery having a cylindrical cell configuration 400. This battery 400 is a lithium-ion (Li-ion) battery. The battery 400 comprises, from its exterior to its core, an enclosure 410, an anode 420, a separator 430, a cathode 440, and a core 450. The battery 400 can be assembled by rolling the enclosure 410 as a set of the cathode 440 (positive electrode; NMC) and the anode 420 (negative electrode; graphite), and the separator 440, into the core 450.

In the respective exemplary embodiment, the enclosure 410 was constructed of an aluminum foil with a thickness of 1 mm. The anode 420 was constructed essentially of graphite. The separator 430 was constructed of polypropylene (PP) with a length of 100 cm for cylindrical cell assembly. The cathode 440 was constructed of the electrode active material as specified in the respective exemplary embodiment and may be coated with a coating material and by the process parameters as specified in the respective exemplary embodiment. And the core 450 was constructed of stainless steel with a dimension of 18 (OD) mm × 17.5 mm (ID) × 67 mm (height).

In each exemplary embodiment, two systems of supercapacitor or battery of same electrode configuration (coin/cylinder) were constructed. The two systems differed in their electrodes. Unless already specified in the above description according to Figs. 1 – 4, the first system was built of the electrode active material as specified in Table 1 or 2 below without any coating (the "reference electrode"); whereas the second system was built similarly to the first system, except that the said electrode active material was coated according to Table 1 or 2 below (the "exemplary electrode").

In an exemplary embodiment where a carbon-based electrode on nickel foam substrate was used as a reference electrode and/or as an electrode active material, the said carbon-based electrode on nickel foam substrate was prepared from a mixture of activated carbon, acetylene black, and polyvinylidene difluoride (PVDF), at the respective weight ratio of 8:8:1. The said mixture solution of the 8:1:1 ratio of activated carbon, acetylene black, and PVDF, of approximately 75 μL was dropped on a nickel foam substrate with an area of 1 cm^2. Next, a nickel foam substrate was baked at 80 °C for 8 hours to remove moisture and allow the dry carbon solution to adhere on the substrate. The nickel foam substrate was then compressed with a pressure of 5 MPa for 1 minute and then weighed to determine the mass of carbon attached on the nickel foam substrate.

In an exemplary embodiment where a lithium-nickel-manganese-cobalt oxide (LiNiMnCoO2, NMC) was used as a reference and/or as an electrode active material, the said NMC had the respective molecular weight ratio of 5:3:2. The NMCs in Exemplary Embodiment No. 1 and 7 were purchased from GELON LIB Group; the NMCs in Exemplary Embodiment Nos. 8 – 11 were purchased from MTI Corporation.

All coatings were applied to the respective electrode active material by sputtering technique. The sputtering source for applying all active coatings was radio frequency (RF) magnetron. The sputtering source for applying all protective coatings was direct current (DC) (if applicable).

In an exemplary embodiment involving supercapacitors, the galvanostatic charge/discharge was measured in an electrolyte comprising 1M of tetraethylammonium tetrafluoroborate (Et4NBF4) in propylene carbonate (PC) with a separator constructed of a cellulose-based paper. The full measurement methodology is set out in Y. Ge et al., *J. Solid State Electrochem*. 24, 3215-3230 (2020) and thus incorporated herein by reference.

In an exemplary embodiment involving batteries, the galvanostatic charge/discharge was measured in an electrolyte comprising 1M of lithium hexafluorophosphate (LiPF6) in ethylene carbonate and diethylene carbonate (EC/DEC) with a separator constructed of polypropylene (PP). The full measurement methodology is set out in Metrohm Autolab 2018, Application Area: Batteries, Galvanostatic charge-discharge of a Li-ion battery with Autolab, Metrohm AN-BAT-002, pp. 1-2, and thus incorporated herein by reference.

In an exemplary embodiment involving the measurement of the thickness of the active coating, the measurement was carried out by the Field Emission Scanning Electron Microscopy (FESEM), operating at 5 kV, using a Hitachi S-4700 and Zeiss AURIGA equipped with an X-ray energy-dispersive spectroscopy (EDS) analyzer.

Table 2 below sets out the specifics of Exemplary Embodiment Nos. 4 – 7 in addition to the preceding general description. Table 3 further below sets out the specifics of Exemplary Embodiment Nos. 8 – 11 in addition to the preceding general description.

Table 2

Exemplary Embodiment No.	4		5		6		7	
A. TYPE OF ENERGY STORAGE DEVICE	Supercapacitor, coin cell		Supercapacitor, coin cell		Supercapacitor, coin cell		Li-ion battery, coin cell	
B. TYPE OF REFERENCE ELECTRODE	Carbon-based		Carbon-based		Carbon-based		NMC	
C. COATING OF EXEMPLARY ELECTRODE	Active coating	Protective coating	Active coating	Protective coating	Active coating	Protective coating	Active coating	Protective coating
(1) Substrate (i.e. electrode active material)	Carbon-based		Carbon-based		Carbon-based		NMC	
(2) Coating material	$BiFeO_3$	N/A	Cu-doped $BiFeO_3$	Cu	Indium-Niobium-doped TiO_2 (InNbTiO2)	Cu	Cu-doped $BiFeO_3$	Cu
(3) Sputtering source	RF		RF	DC	RF	DC	RF	DC
(4) Operating pressure (Pa)	0.4 ± 0.3		1.4 ± 0.3	1.0 ± 0.2	1.9 ± 0.3	1.1 ± 0.2	1.4 ± 0.3	1.0 ± 0.2
(5) Power (W)	100		100	20	100	20	100	20
(6) Flow rate of the reactive gas (Ar:O2) (sccm)	16:4		12:4	5:0	12:4	5:0	12:4	5:0
(7) Deposition time (minutes)	1		30	2	30	2	30	2
(8) Substrate temperature (°C)	RT		RT	RT	RT	RT	RT	RT
(9) Thickness (nm)	7		200	N/A	200	N/A	200	N/A
D. GALVANOSTATIC CHARGE/DISCHARGE PARAMETERS								
(1) Current density (A/g)	0.1		0.1		0.1		0.035	
(2) Voltage (V)	0.5 - 3.0		0.25 - 2.6		0.8 - 2.6		3.0 - 4.2	

Table 3

Exemplary Embodiment No.	8		9		10		11	
A. TYPE OF ENERGY STORAGE DEVICE	Li-ion battery, coin cell		Li-ion battery, coin cell		Li-ion battery, coin cell		Li-ion battery, coin cell	
B. TYPE OF REFERENCE ELECTRODE	NMC		NMC		NMC		NMC	
C. COATING OF EXEMPLARY ELECTRODE	Active coating	Protective coating	Active coating	Protective coating	Active coating	Protective coating	Active coating	Protective coating
(1) Substrate (i.e. electrode active material)	NMC		NMC		NMC		NMC	
(2) Coating material	Cu-doped BiFeO3	Cu	BiFeO3	Cu	BaTiO3	Cu	NiO	N/A
(3) Sputtering source	RF	DC	RF	DC	RF	DC	RF	
(4) Operating pressure (Pa)	1.4 ± 0.3	1.0 ± 0.2	0.8 ± 0.3	1.0 ± 0.2	1.8 ± 0.3	0.5 ± 0.2	2.9 ± 0.4	
(5) Power (W)	100	20	100	20	100	20	100	
(6) Flow rate of the reactive gas (Ar:O2) (sccm)	12:4	5:0	16:4	5:0	12:4	5:0	20:20	
(7) Deposition time (minutes)	1	2	0.27	2	15	2	30	
(8) Substrate temperature (°C)	RT	RT	RT	RT	RT	RT	RT	
(9) Thickness (nm)	7	N/A	7	N/A	122	N/A	200	
D. GALVANOSTATIC CHARGE/DISCHARGE PARAMETERS								
(1) Current density (A/g)	0.035		0.035		0.035		0.035	
(2) Voltage (V)	3.0 - 4.2		3.0 - 4.2		0.5 - 3.0		0.0 - 3.0	

Results Discussion

Exemplary Embodiment No. 1

Fig. 5 shows the change of voltage (V) over time (minutes) of an NMC electrode coated with an active coating comprising Cu-doped $BiFeO_3$ according to Exemplary Embodiment No. 1. Between the voltage of 4.05 – 4.12 V of its charging phase, the exemplary electrode exhibited a negative slope representing the rate of -0.006 V/min. The electric current was kept constant at 0.98 mA throughout the charge/discharge cycle, including the time in which the negative rate was observed (110 – 145 minutes of the charging phase). Thus, the change of slope was determined to be -0.102 V/Coulomb; and the negative rate of μ over n was determined to be (-0.102 V/Coulomb $\times$ (1.6×10^{-19} Coulomb) $\times$ 10^3) $\times$ (0.028 g $\times$ 649 $m^2/g \times 10^4$) = - 2.97×10^{-12} millielectronvolt per electron per cm^2, where 1.6×10^{-19} Coulomb was the charge of an electron, 0.028 g was the mass of active material, and 649 m^2/g was the specific surface area of the NMC electrode. In contrast to the exemplary electrode, the reference electrode showed a positive slope through the charging phase at the rate of 0.004 V/min. The change of slope was determined to be 0.068 V/Coulomb. The rate of μ over n was thus determined to be (0.068 V/Coulomb $\times$ (1.6×10^{-19} Coulomb) $\times$ 10^3) $\times$ (0.028 g $\times$ 649 $m^2/g \times 10^4$) = 1.977×10^{-12} millielectronvolt per electron per cm^2.The negative rate of μ over n, as observed from the said negative slope, promoted the electrode's energy density and thus electrical capacity, as will be shown and discussed with respect to later exemplary embodiments.

Exemplary Embodiment No. 2

According to Exemplary Embodiment No. 2, Fig. 6A shows the change of the chemical potential μ as a function of the electron density *n2D* of the exemplary electrode; Fig. 6B shows the rate of change of the chemical potential over the electron density ($d\mu/dn$) as a function of the electron density *n2D* of the exemplary electrode. From these two Figures, the negative rate of μ over n, which was calculated in Exemplary Embodiment No. 1, may be directly measured by ultraviolet photoemission spectroscopy (UPS). The electronic structure of $BiFeO_3$ measured by UPS was performed using Scienta R4000 electron analyzer located at Beamline 10.0.1 Advanced Light Source (USA) and Beamline 3.2a of the Synchrotron Light Research Institute, Thailand. The measurements were performed at room temperature with base pressure better than 5×10^{-8} mbar and the photon energy was set to be 60 eV. Here, the negative chemical potential shift indicated a

counterintuitive lowering of the chemical potential with increasing electron densities, which was a direct spectroscopic signature of the negative electron compressibility (NEC).

According to Figs. 6A and 6B, the negative rate of μ over n resulting from the Exemplary Embodiment No. 2 was determined to be in the range of -2.34×10^{-8} to -5.39×10^{-8} millielectronvolt per electron per cm^2.

Exemplary Embodiment No. 3

Fig. 7 shows the percentage of energy density increased in Li-ion battery-based lithium-nickel-manganese-cobalt oxide ($LiNiMnCoO_2$, NMC) electrode coated with Cu-doped $BiFeO_3$ thin film presented as a function of thickness. Here, the increased energy density was measured relative to the active coating's thicknesses of 3.5 – 34 nm. A remarkably high percentage of the increase of energy density was observed at the active coating's thicknesses of 3.5 – 14.0 nm. This indicated that within the working thickness range, a thin active coating provides a better energy density than a thick active coating.

Exemplary Embodiment No. 4

Figs. 8A and 8B show, respectively, the change of voltage (V) over time (minutes) and the change of energy density (Wh/kg) over cycles of charge/discharge, of a supercapacitor comprising reference electrodes and another supercapacitor comprising electrodes according to Exemplary Embodiment No. 4.

According to Fig. 8A, at a constant current density of 0.1 A/g, the supercapacitor comprising the exemplary electrodes exhibited a significantly longer time to charge to, and discharge from, the discharge/charge voltages of 3 V. The area under the curve of voltage over time was positively proportional to energy capacity. Thus, the supercapacitor comprising the exemplary electrodes had a greater energy capacity than the supercapacitor comprising the reference electrodes.

According to Fig. 8B, the supercapacitor comprising the exemplary electrodes exhibited an energy density that was about 100 % greater than the supercapacitor comprising the reference electrodes. In particular, the supercapacitor comprising exemplary electrodes exhibited an energy density of 8 ± 0.1 Wh/kg; the supercapacitor comprising reference electrodes exhibited an energy density of 4 ± 0.1 Wh/kg. This superiority in the energy capacity was retained after the 10^{th} charge/discharge cycle.

Exemplary Embodiment No. 5

Figs. 9A and 9B show, respectively, the change of voltage (V) over time (minutes) and the change of energy density (Wh/kg) over cycles of charge/discharge, of a supercapacitor comprising reference electrodes and another supercapacitor comprising electrodes according to Exemplary Embodiment No. 5.

According to Fig. 9A, at a constant current density of 0.1 A/g, the supercapacitor comprising the exemplary electrodes exhibited a significantly longer time to charge to, and discharge from, the discharge/charge voltages of 2.5 – 2.6 V. The area under the curve of voltage over time was positively proportional to energy capacity. Thus, the supercapacitor comprising the exemplary electrodes had a greater energy capacity than the supercapacitor comprising the reference electrodes.

According to Fig. 9B, the supercapacitor comprising the exemplary electrodes exhibited an energy density that was about 29 % greater than the supercapacitor comprising the reference electrodes. In particular, the supercapacitor comprising exemplary electrodes exhibited an energy density of 16.4 ± 0.1 Wh/kg; the supercapacitor comprising reference electrodes exhibited an energy density of 12.7 ± 0.1 Wh/kg. This superiority in the energy capacity was retained after the 10^{th} charge/discharge cycle.

Exemplary Embodiment No. 6

Figs. 10A and 10B show, respectively, the change of voltage (V) over time (minutes) and the change of energy density (Wh/kg) over cycles of charge/discharge, of a supercapacitor comprising reference electrodes and another supercapacitor comprising electrodes according to Exemplary Embodiment No. 6.

According to Fig. 10A, at a constant current density of 0.1 A/g, the supercapacitor comprising the exemplary electrodes exhibited a significantly longer time to charge to, and discharge from, the discharge/charge voltages of 2.6 V. The area under the curve of voltage over time was positively proportional to energy capacity. Thus, the supercapacitor comprising the exemplary electrodes had a greater energy capacity than the supercapacitor comprising the reference electrodes.

According to Fig. 10B, the supercapacitor comprising the exemplary electrodes exhibited an energy density that was about 46 % greater than the supercapacitor comprising the reference electrodes. In particular, the supercapacitor comprising exemplary electrodes exhibited an energy density of 13 ± 0.1 Wh/kg; the supercapacitor comprising reference electrodes exhibited an energy

density of 9 ± 0.1 Wh/kg. This superiority in the energy capacity was retained after the 10th charge/discharge cycle.

Exemplary Embodiment No. 7

Figs. 11A and 11B show, respectively, the change of voltage (V) over time (minutes) and the change of energy density (Wh/kg) over cycles of charge/discharge, of a lithium-ion battery comprising reference electrodes and another lithium-ion battery comprising electrodes according to Exemplary Embodiment No. 7.

According to Fig. 11A, at a constant current density of 0.035 A/g, the battery comprising the exemplary electrodes exhibited a significantly longer time to charge to, and discharge from, the discharge/charge voltages of 4.2 V. The area under the curve of voltage over time was positively proportional to energy capacity. Thus, the battery comprising the exemplary electrodes had a greater energy capacity than the battery comprising the reference electrodes.

According to Fig. 11B, the battery comprising the exemplary electrodes exhibited an energy density that was about 22 % greater than the battery comprising the reference electrodes. In particular, the battery comprising exemplary electrodes exhibited an energy density of 275 ± 5 Wh/kg; the battery comprising reference electrodes exhibited an energy density of 225 ± 5 Wh/kg. This superiority in the energy capacity was retained after the 10th charge/discharge cycle.

Exemplary Embodiment No. 8

Figs. 12A and 12B show, respectively, the change of voltage (V) over time (minutes) and the change of energy density (Wh/kg) over cycles of charge/discharge, of a lithium-ion battery comprising reference electrodes and another lithium-ion battery comprising electrodes according to Exemplary Embodiment No. 8.

According to Fig. 12A, at a constant current density of 0.035 A/g, the battery comprising the exemplary electrodes exhibited a significantly longer time to charge to, and discharge from, the discharge/charge voltages of 4.2 V. The area under the curve of voltage over time was positively proportional to energy capacity. Thus, the battery comprising the exemplary electrodes had a greater energy capacity than the battery comprising the reference electrodes.

According to Fig. 12B, the battery comprising the exemplary electrodes exhibited an energy density that was about 8 % greater than the battery comprising the reference electrodes. In particular, the battery comprising exemplary electrodes exhibited an energy density of 334 ± 5 Wh/kg; the

battery comprising reference electrodes exhibited an energy density of 315 ± 5 Wh/kg. This superiority in the energy capacity was retained after the 10th charge/discharge cycle.

Exemplary Embodiment No. 9

Figs. 13A and 13B show, respectively, the change of voltage (V) over time (minutes) and the change of energy density (Wh/kg) over cycles of charge/discharge, of a lithium-ion battery comprising reference electrodes and another lithium-ion battery comprising electrodes according to Exemplary Embodiment No. 9.

According to Fig. 13A, at a constant current density of 0.035 A/g, the battery comprising the exemplary electrodes exhibited a significantly longer time to charge to, and discharge from, the discharge/charge voltages of 4.2 V. The area under the curve of voltage over time was positively proportional to energy capacity. Thus, the battery comprising the exemplary electrodes had a greater energy capacity than the battery comprising the reference electrodes.

According to Fig. 13B, the battery comprising the exemplary electrodes exhibited an energy density that was about 3 % greater than the battery comprising the reference electrodes. In particular, the battery comprising exemplary electrodes exhibited an energy density of 278 ± 5 Wh/kg; the battery comprising reference electrodes exhibited an energy density of 270 ± 5 Wh/kg. This superiority in the energy capacity was retained after the 10th charge/discharge cycle.

Comparison between the above-described exemplary electrode of Exemplary Embodiment No. 8 (exhibiting an energy density of 334 ± 5 Wh/kg) and the exemplary electrode of Exemplary Embodiment No. 9 (exhibiting an energy density of 278 ± 5 Wh/kg) confirms that a five-percent doping of Cu into $BiFeO_3$ active coating (No. 8) yielded a greater energy density than $BiFeO_3$ active coating without metal dopant (No. 9).

Exemplary Embodiment No. 10

Figs. 14A and 14B show, respectively, the change of voltage (V) over time (minutes) and the change of energy density (Wh/kg) over cycles of charge/discharge, of a lithium-ion battery comprising reference electrodes and another lithium-ion battery comprising electrodes according to Exemplary Embodiment No. 10.

According to Fig. 14A, at a constant current density of 0.035 A/g, the battery comprising the exemplary electrodes exhibited a significantly longer time to charge to, and discharge from, the discharge/charge voltages of 3.0 V. The area under the curve of voltage over time was positively

proportional to energy capacity. Thus, the battery comprising the exemplary electrodes had a greater energy capacity than the battery comprising the reference electrodes.

According to Fig. 14B, the battery comprising the exemplary electrodes exhibited an energy density that was about 31 % greater than the battery comprising the reference electrodes. In particular, the battery comprising exemplary electrodes exhibited an energy density of 21 ± 5 Wh/kg; the battery comprising reference electrodes exhibited an energy density of 16 ± 5 Wh/kg. This superiority in the energy capacity was retained after the 10^{th} charge/discharge cycle.

Exemplary Embodiment No. 11

Figs. 15A and 15B show, respectively, the change of voltage (V) over time (minutes) and the change of energy density (Wh/kg) over cycles of charge/discharge, of a lithium-ion battery comprising reference electrodes and another lithium-ion battery comprising electrodes according to Exemplary Embodiment No. 11.

According to Fig. 15A, at a constant current density of 0.035 A/g, the battery comprising the exemplary electrodes exhibited a significantly longer time to charge to, and discharge from, the discharge/charge voltages of 3.0 V. The area under the curve of voltage over time was positively proportional to energy capacity. Thus, the battery comprising the exemplary electrodes had a greater energy capacity than the battery comprising the reference electrodes.

According to Fig. 15B, the battery comprising the exemplary electrodes exhibited an energy density that was about 44 % greater than the battery comprising the reference electrodes. In particular, the battery comprising exemplary electrodes exhibited an energy density of 23 ± 5 Wh/kg; the battery comprising reference electrodes exhibited an energy density of 16 ± 5 Wh/kg. This superiority in the energy capacity was retained after the 10^{th} charge/discharge cycle.

In summary, the coating of Cu-doped BFO thin film was applied on the electrodes of supercapacitors and lithium-ion batteries by using sputtering technique. When galvanostatic charge/discharge were measured, the capacity enhancements were clearly observed on the supercapacitors and lithium-ion batteries with the coated electrodes. With the Cu-doped BFO thin film, the retention performance became better than the original supercapacitors and lithium-ion batteries without the coating of Cu-doped BFO thin film and the protective coating.

List of Drawing References

100 Supercapacitor, coin cell

112 Positive cap
114 Cathode spring
116 Cathode spacer
118 Cathode
120 Separator
132 Anode
134 Anode spacer
136 Negative cap
200 Supercapacitor, cylindrical cell
210 Enclosure
220 Anode
230 Separator
240 Cathode
250 Core
300 Battery, coin cell
312 Positive cap
314 Cathode spring
316 Cathode spacer
318 Cathode
320 Separator
332 Anode
334 Anode spacer
336 Negative cap
400 Battery, cylindrical cell
410 Enclosure
420 Anode
430 Separator
440 Cathode
450 Core

CLAIMS

1. An active coating of an electrode active material, said active coating having a thickness of 1 nanometer – 1 micrometer and comprising a transition metal oxide, said active coating imparting, to the electrode active material upon which said active coating is deposited, a negative rate of μ over n, wherein:
   said μ represents a chemical potential;
   said n represents a number of electrons per a unit area; and
   said negative rate is between 0 and -5.39×10^{-8} millielectronvolt per electron per cm^2.

2. The active coating according to Claim 1 having a thickness of 3.5 – 14.0 nanometers.

3. The active coating according to Claim 1, wherein said transition metal oxide is doped with at least one metal dopant.

4. The active coating according to Claim 3, wherein said metal dopant is a transition metal element.

5. The active coating according to Claim 3, wherein said metal dopant is a post-transition metal element.

6. The active coating according to Claim 3, wherein said metal dopant is selected from a group of niobium (Nb), indium (In), and copper (Cu).

7. The active coating according to Claim 1, wherein the transition metal oxide is selected from a group of bismuth ferrite ($BiFeO_3$), nickel (II) oxide (NiO), and barium titanate (BaTiO3).

8. The active coating according to Claim 3, wherein the transition metal oxide that is doped with at least one metal dopant is $Bi_{0.80-0.95}\ Cu_{0.05-0.10}\ FeO_3$.

9. The active coating according to Claim 3, wherein the doping is carried out in order to optimize the negative rate of μ over n, such that said negative rate of μ over n corresponds to a host energy storage where the coating is applied.

10. The active coating according to Claim 1 that is applied to the electrode active material by physical vapor deposition.

11. The active coating of the electrode active material of a battery, said active coating being in accordance with any one of Claim 1 – 10.

12. The active coating of the electrode active material of a supercapacitor, said active coating being in accordance with any one of Claim 1 – 10.

13. The energy storage device comprising the electrode active material upon which the active coating according to any one of Claim 1 – 10 is deposited.

14. The energy storage device according to Claim 13 that is a coin cell of a supercapacitor or a battery.

15. The energy storage device according to Claim 13 that is a cylindrical cell of a supercapacitor or a battery.

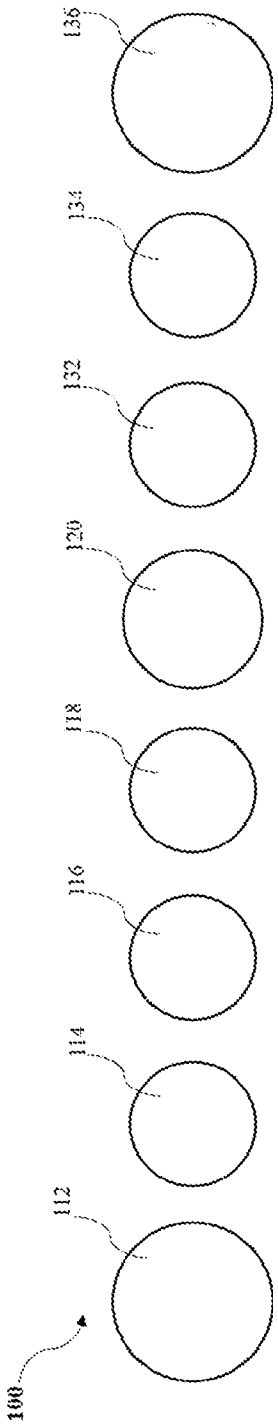

FIG. 1

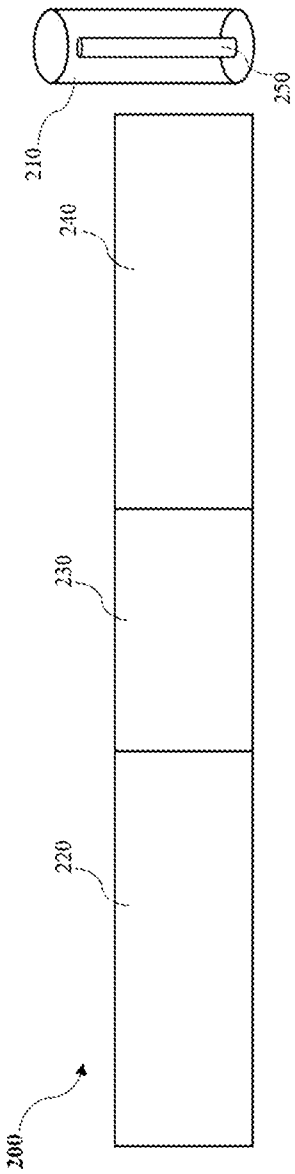

FIG. 2

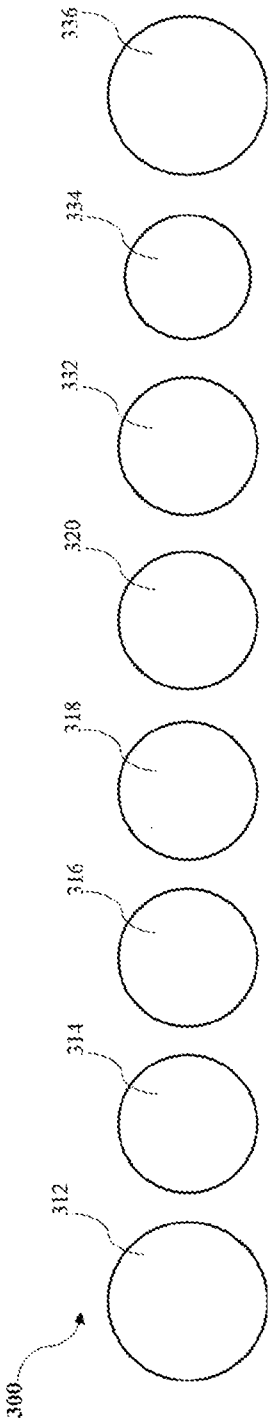

FIG. 3

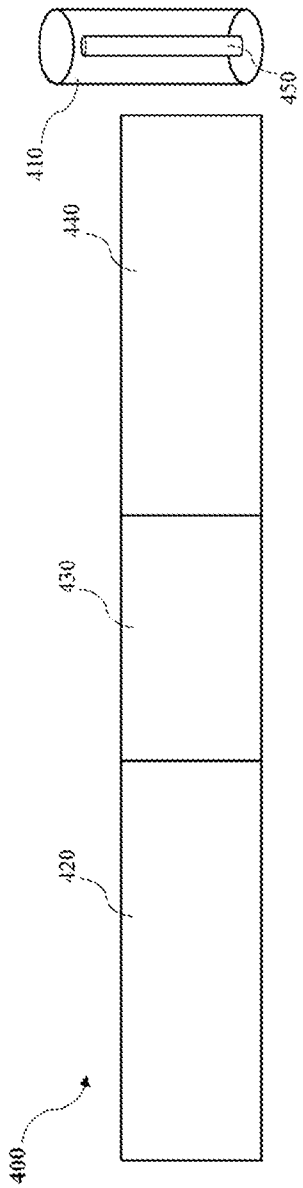

FIG. 4

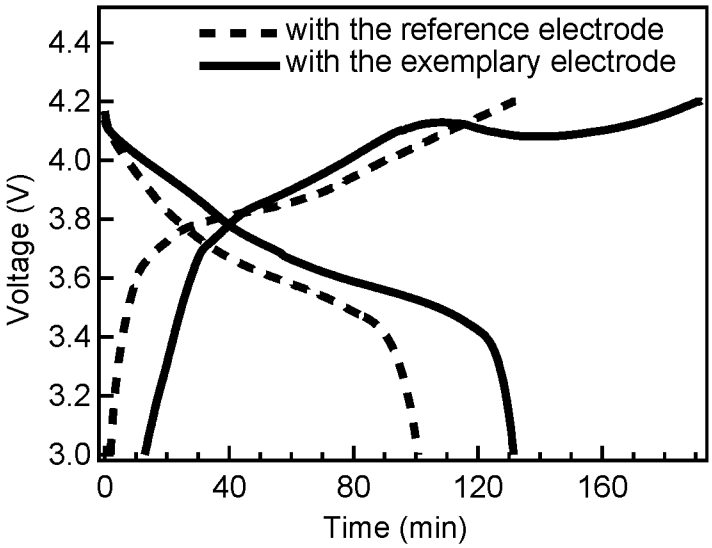
with the reference electrode
with the exemplary electrode
Voltage (V)
Time (min)
4.4
4.2
4.0
3.8
3.6
3.4
3.2
3.0
0
40
80
120
160

FIG. 5

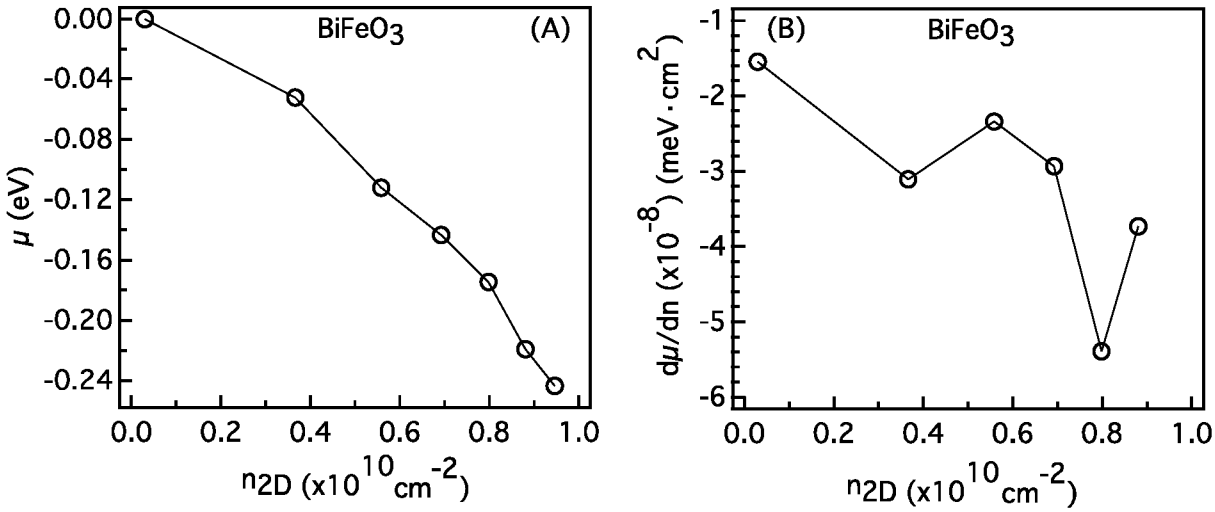
BiFeO3
(A)
μ (eV)
n2D (x10^10 cm^-2)
0.00
-0.04
-0.08
-0.12
-0.16
-0.20
-0.24
0.0
0.2
0.4
0.6
0.8
1.0
(B)
BiFeO3
dμ/dn (x10^-8) (meV·cm^2)
-1
-2
-3
-4
-5
-6

FIG. 6

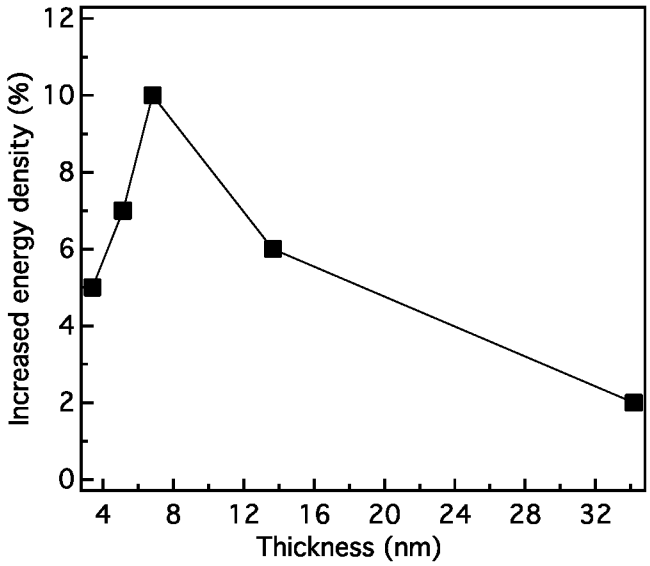
Increased energy density (%)
Thickness (nm)
0
2
4
6
8
10
12
4
8
12
16
20
24
28
32

FIG. 7

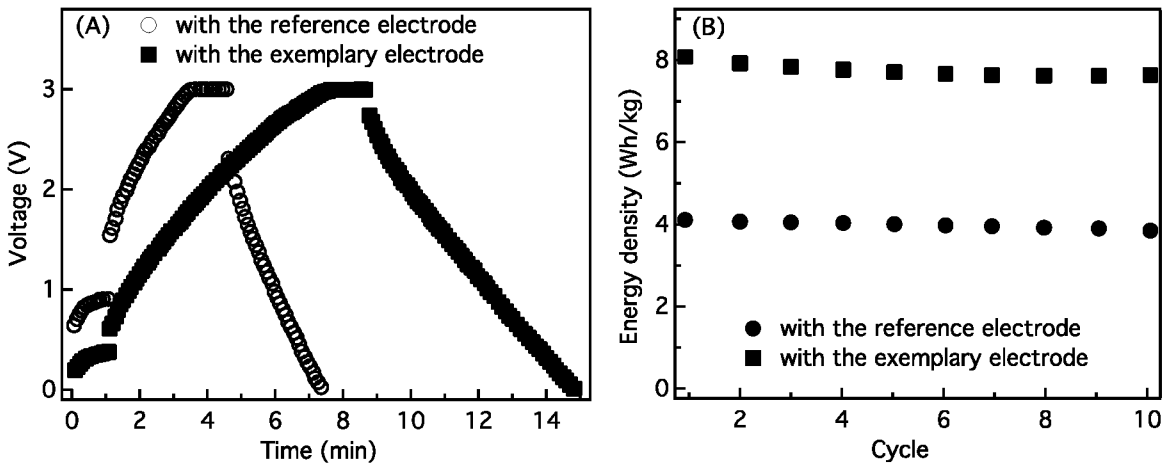
(A)
with the reference electrode
with the exemplary electrode
Voltage (V)
Time (min)
(B)
Energy density (Wh/kg)
Cycle
with the reference electrode
with the exemplary electrode

FIG. 8

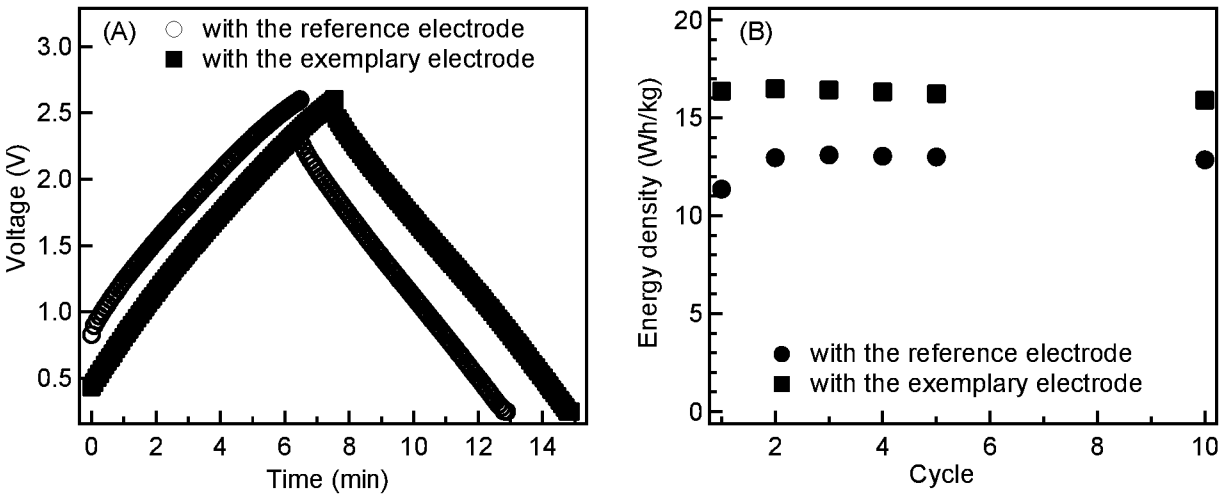
(A)
with the reference electrode
with the exemplary electrode
Voltage (V)
Time (min)
(B)
Energy density (Wh/kg)
Cycle
with the reference electrode
with the exemplary electrode

FIG. 9

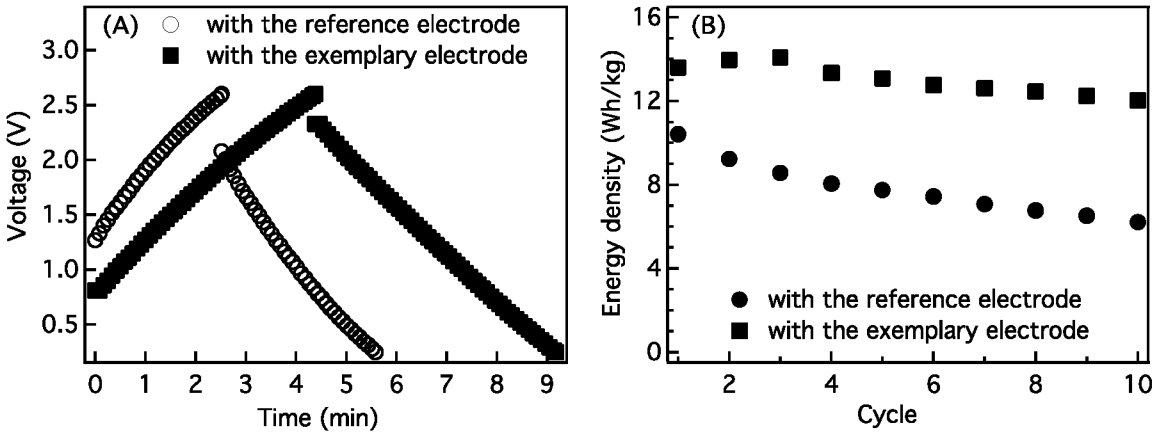
(A)
with the reference electrode
with the exemplary electrode
Voltage (V)
Time (min)
(B)
Energy density (Wh/kg)
Cycle
with the reference electrode
with the exemplary electrode

FIG. 10

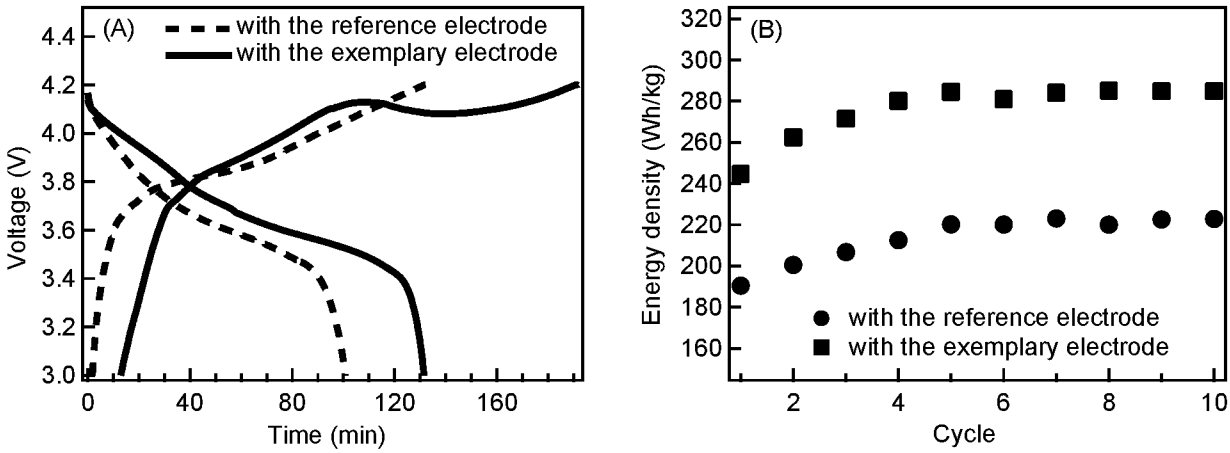
(A)
with the reference electrode
with the exemplary electrode
Voltage (V)
Time (min)
(B)
Energy density (Wh/kg)
Cycle
with the reference electrode
with the exemplary electrode

FIG. 11

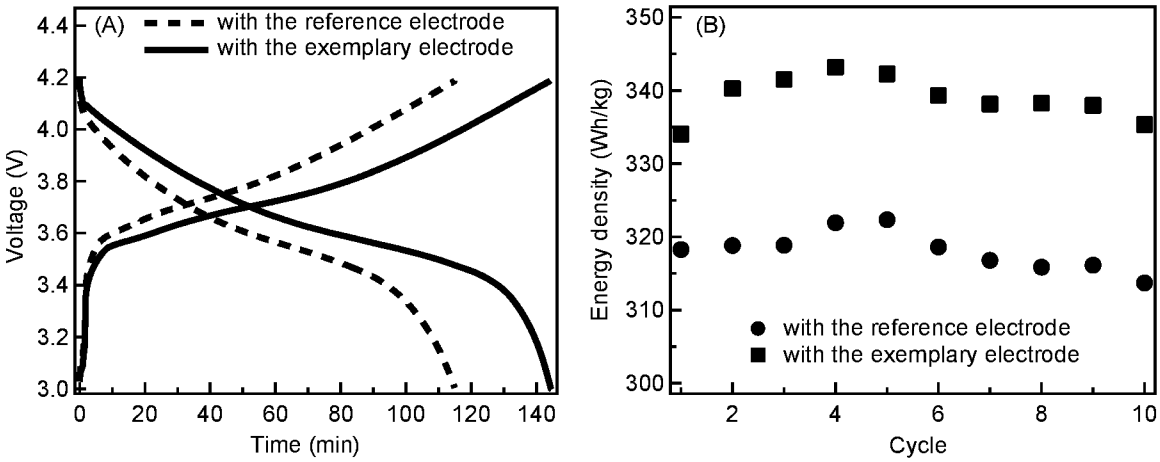
(A)
with the reference electrode
with the exemplary electrode
Voltage (V)
Time (min)
(B)
Energy density (Wh/kg)
Cycle
with the reference electrode
with the exemplary electrode

FIG. 12

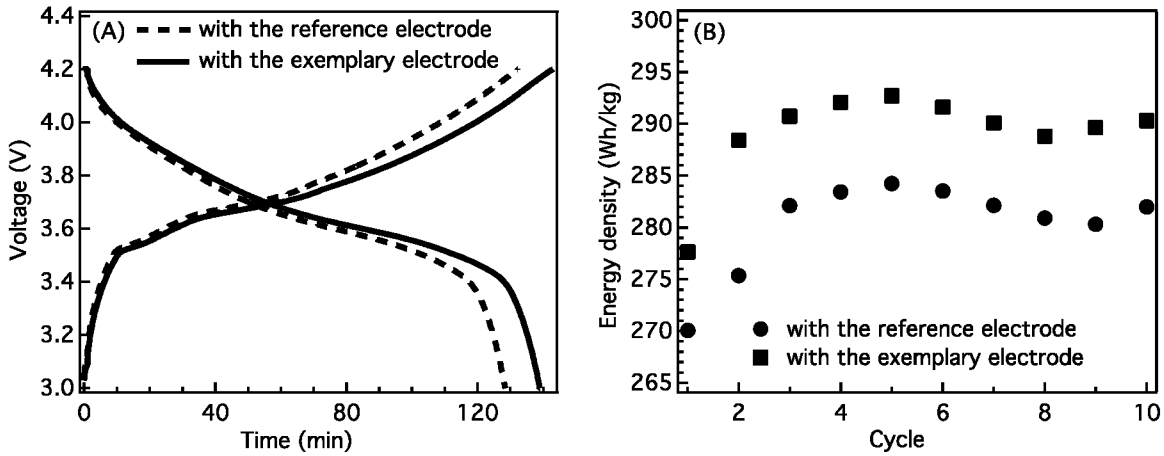
(A)
with the reference electrode
with the exemplary electrode
Voltage (V)
Time (min)
(B)
Energy density (Wh/kg)
Cycle
with the reference electrode
with the exemplary electrode

FIG. 13

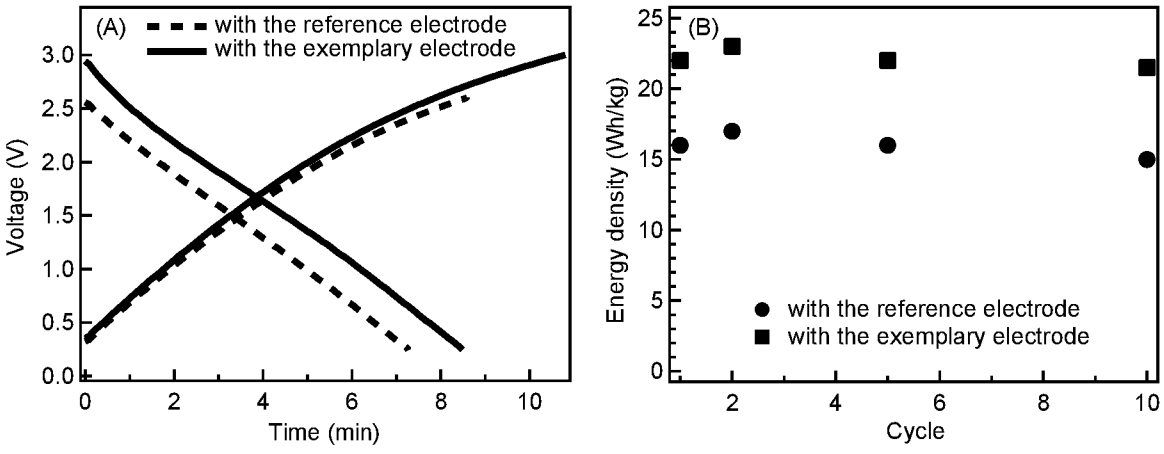
(A)
with the reference electrode
with the exemplary electrode
Voltage (V)
Time (min)
(B)
Energy density (Wh/kg)
Cycle
with the reference electrode
with the exemplary electrode

FIG. 14

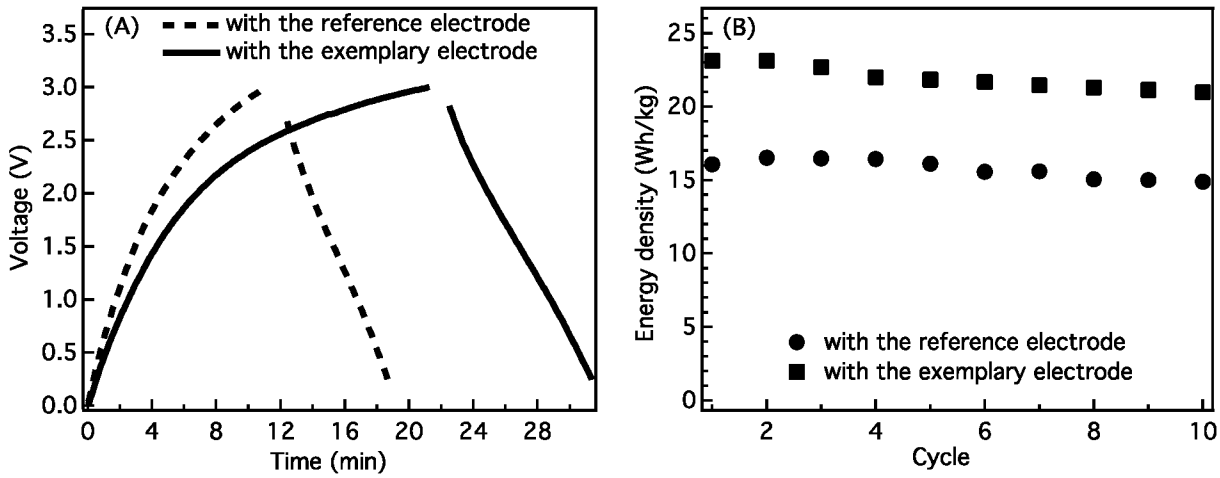
(A)
with the reference electrode
with the exemplary electrode
Voltage (V)
Time (min)
(B)
Energy density (Wh/kg)
Cycle
with the reference electrode
with the exemplary electrode

FIG. 15